Human Molecular Genetics, 2010, Vol. 19, No. 21 ***4239–4252***
doi:10.1093/hmg/ddq343
Advance Access published on August 12, 2010

A humanized *Smn* gene containing the *SMN2* nucleotide alteration in exon 7 mimics *SMN2* splicing and the SMA disease phenotype

Jordan T. Gladman[1,2], Thomas W. Bebee[1,3], Chris Edwards[1], Xueyong Wang[4], Zarife Sahenk[1], Mark M. Rich[4] and Dawn S. Chandler[1,2,3,*]

[1]Department of Pediatrics, The Research Institute at Nationwide Children's Hospital, [2]The Integrated Biomedical Science Graduate Program (IBGP) and [3]The Molecular, Cellular and Developmental Biology (MCDB) Graduate Program, The Ohio State University, Columbus, OH, USA and [4]Department of Neuroscience, Cell Biology, and Physiology, Wright State University, Dayton, OH, USA

Received July 15, 2010; Revised July 15, 2010; Accepted August 9, 2010

Proximal spinal muscular atrophy (SMA) is a neurodegenerative disease caused by low levels of the survival motor neuron (SMN) protein. In humans, *SMN1* and *SMN2* encode the SMN protein. In SMA patients, the *SMN1* gene is lost and the remaining *SMN2* gene only partially compensates. Mediated by a C>T nucleotide transition in *SMN2*, the inefficient recognition of exon 7 by the splicing machinery results in low levels of SMN. Because the *SMN2* gene is capable of expressing SMN protein, correction of *SMN2* splicing is an attractive therapeutic option. Although current mouse models of SMA characterized by *Smn* knock-out alleles in combination with *SMN2* transgenes adequately model the disease phenotype, their complex genetics and short lifespan have hindered the development and testing of therapies aimed at *SMN2* splicing correction. Here we show that the mouse and human minigenes are regulated similarly by conserved elements within in exon 7 and its downstream intron. Importantly, the C>T mutation is sufficient to induce exon 7 skipping in the mouse minigene as in the human *SMN2*. When the mouse *Smn* gene was humanized to carry the C>T mutation, keeping it under the control of the endogenous promoter, and in the natural genomic context, the resulting mice exhibit exon 7 skipping and mild adult onset SMA characterized by muscle weakness, decreased activity and an alteration of the muscle fibers size. This *Smn* C>T mouse represents a new model for an adult onset form of SMA (type III/IV) also know as the Kugelberg–Welander disease.

INTRODUCTION

Proximal spinal muscular atrophy (SMA) is a disease characterized by the loss of alpha-motor neurons resulting in progressive muscle atrophy, which leads to paralysis and death. SMA occurs in approximately 1 in 10 000 live births (1). It was found that SMA occurs when there is a homozygous loss of the *Survival Motor Neuron 1* (*SMN1*) gene located on chromosome 5q13 (2).

SMN2, a nearly identical gene also located on chromosomal segment 5q13, can produce the same protein generated by *SMN1* (2). This is due to the small number of nucleotide differences between *SMN1* and *SMN2*, most of which have been shown to have no effect on *SMN* levels or protein function due to their location in the introns. However *SMN2*'s translationally silent T at nucleotide +6 of exon 7 instead of *SMN1*'s C causes the final RNA product to be improperly regulated. In *SMN2*, the majority of the pre-mRNA transcripts generated results in transcripts lacking exon 7. *SMN2* does, however, produce a small amount of full-length transcript and thus full-length protein (3,4). Improper regulation of the *SMN2* gene occurs because the C>T alteration disrupts the binding of the exonic splicing enhancer SF2/ASF and creates the exonic splicing silencer hnRNP A1 binding site (5,6). Additionally the 5′ splice site is inefficient, due to a non-wild-type guanosine residue alteration (A54G). When

*To whom correspondence should be addressed at: Center for Childhood Cancer, WA5023, The Research Institute at Nationwide Children's Hospital, 700 Children's Drive, Columbus, OH 43205, USA. Tel: +1 6147225598; Fax: +1 6147225895; Email: chandler.135@osu.edu

© *The Author 2010. Published by Oxford University Press. All rights reserved.*
For Permissions, please email: journals.permissions@oxfordjournals.org

Downloaded from https://academic.oup.com/hmg/article/19/21/4239/666050 by guest on 09 April 2024

combined with the already identified suboptimal 5′ and 3′ splice site present in exon 7, the C>T disruption of the SF2/ASF site results in the poor recognition of exon 7 in the *SMN2* gene (7).

Severe disease symptoms occur with lower levels of SMN protein, and complete absence of the *Smn* gene is embryonic lethal in mice underscoring the role of functional SMN protein in disease severity (8–11). The presence of *SMN2* gene in patients with SMA offers a unique therapeutic point of intervention. Therapies aimed at producing more functional full-length transcript from the *SMN2* gene have the potential to be a viable treatment of SMA.

Whereas the SMN protein is present in all vertebrate species, only humans have both *SMN1* and *SMN2* genes. The mouse *Smn* gene was identified in 1997 and found to be located on chromosome 13 in a region syntenic to that of human chromosome 5q13 where the human *SMN1* and *SMN2* genes are located (12). Mice have only one *Smn* gene, which produces full-length constitutively spliced mRNA product, as it lacks the C>T alteration present in *SMN2*. However, the mouse and human exon 7 share a high level of nucleotide (81%) and amino acid (75%) identity (12,13).

There are a number of animal models currently available to examine SMN protein levels and *SMN*2 splicing in SMA (14,15). Currently, the most common mouse models of SMA have short lifespans of 0–15 days and require following multiple genomic loci (11,16,17). Others models have longer lifespans but use SMA patient mutations that modify protein function, such as the *SMN1* A2G missense mutation (18), or mutations in the *Smn* allele that disrupt splicing in a fashion not observed in the *SMN2* gene (19,20). Both of these alterations can complicate testing therapies aimed at splicing correction. Although much of the work in understanding *SMN* and its role in SMA has been done using the currently available models, and innovative breeding strategies have been utilized to make generating the desired genotypes of these mice easier (21), their short lifespan still provides a difficulty in testing therapeutic compounds. Generating a new SMA model with a milder juvenile or adult onset disease phenotype using the mouse genomic locus would help in the understanding and treatment of SMA and simplify the genetics required to conduct research.

We propose generating a new model of SMA using the endogenous mouse *Smn* gene and homologous recombination to insert the C>T *SMN2* alteration into exon 7. Using comparative genomics and an *in vivo* splicing assay, we demonstrate that the mouse *Smn* and human *SMN* genes are regulated at exon 7 by many of the same pre-mRNA splicing elements. Furthermore, when the C>T alteration in exon 7 of the *SMN2* gene is engineered into the mouse *Smn* gene, we see increases in exon 7 pre-mRNA skipping. By using homologous recombination, the modified *Smn* C>T allele is under the endogenous *Smn* promoter and in the correct genomic context. Biochemical, histological and behavioral analysis of the resultant mice are consistent with a mild adult onset form of SMA including reduced hindlimb grip strength and decreased locomotive activity along with hypertrophic skeletal muscle fibers as seen in some Kugelberg–Welander SMA patients. The lifespan of our mice is extended and allows treatment of the disease at later developmental time points, beyond which other SMA mouse models do not survive. This model thus has the benefit of adding to the spectrum of SMA animal models available and allows for the testing for modifiers of disease phenotype and development of therapies that directly affect exon 7 splicing.

RESULTS

Splicing regulation of mouse and human *Survival Motor Neuron* genes

The purpose of the research described here is to design a new mouse model for SMA using homologous recombination to insert the *SMN2* C>T nucleotide alteration into the endogenous mouse *Smn* gene. However, before generating this animal, we wanted to determine whether the mouse *Smn* gene is regulated in a manner similar to the human *SMN* genes. The mouse *Smn* gene has an 83% nucleotide identity in the open-reading frame when compared with the human sequence (12,13). To determine whether the regulation between the two species was similar, we generated wild-type mouse *Smn* and human *SMN1* and *SMN2* minigenes from genomic DNA. Next we used site-directed mutagenesis to introduce the *SMN2* C>T point mutation into the mouse pSmnWT and human pSMN1 minigenes. These mouse and human minigene constructs contain exons 6–8 and all intervening sequences (Fig. 1A). The expression vectors were sequenced to confirm the correct DNA sequence. We then compared the splicing profile of our minigenes to determine what effect the C>T point mutation had on the regulated splicing of the mouse *Smn* gene by transfecting each minigene (pSMN1, pSMNC>T, pSmnWT and pSmnC>T) into the HEK 293T cell line and analyzing the splicing products using RT–PCR. Both mouse pSmnWT and human pSMN1 minigenes produced full-length transcripts as expected. Additionally, similar to what has been observed in the *SMN2* gene, the presence of the C>T point mutation in the mouse *Smn* and human *SMN1* minigenes caused an increase in transcripts lacking exon 7 (Fig. 1B).

Comparisons of the spliced transcripts generated from transfecting the mouse pSmnC>T and human pSMNC>T into the HEK 293T observed on average 65.6 ± 6.2% skipped product in the mouse minigene and 69.3 ± 6.6% skipped product in the human minigene (Fig. 1B and Supplementary Material, Fig. S1a). In both cases, the C>T point mutation resulted in similar levels of exon 7 skipping and this splicing phenotype was observed in multiple cell lines (Supplementary Material, Fig. S1b). Unlike previous findings using mouse minigenes (22), the splicing found in our mouse minigenes did not use any cryptic splice site located in exon 8 and showed a greater degree of skipped transcript that more closely mimics the splicing of the *SMN2* gene.

In an attempt to explain this inconsistency, we examined the sequences used in the DiDonato minigenes. They found that exon 8, which lies outside the coding nucleotides of the mouse gene, contained a 45-nucleotide repeat which was not present in the human genes (12,13,22). However, this original sequencing was done using the BAC20g19 construct and not directly from the genomic DNA; thus, the 45-nucleotide

Downloaded from https://academic.oup.com/hmg/article/19/21/4239/666050 by guest on 09 April 2024

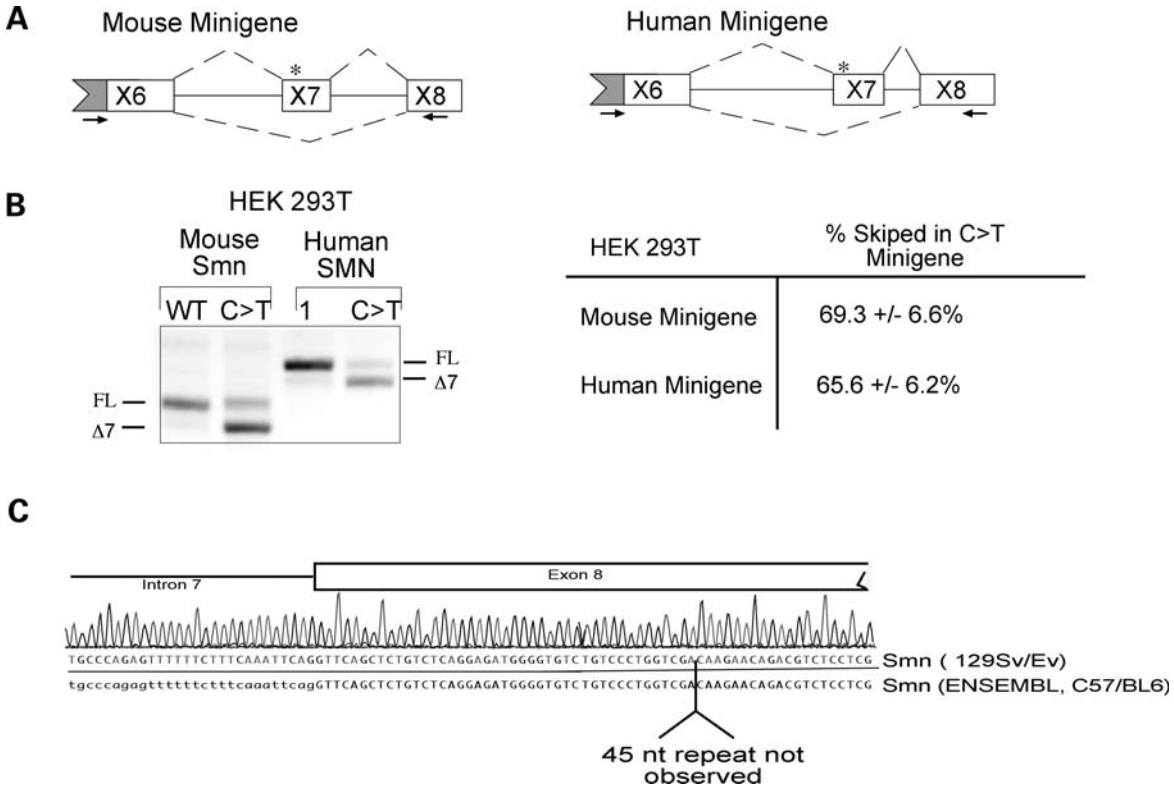

Figure 1. Mouse and human minigenes show similar pre-mRNA splicing. (**A**) Schematic representation of the mouse *Smn* and human *SMN1* minigenes generated with primers represented by the arrows present in the vector-specific FLAG tag or exon 8. The asterisk represents the exon 7 ESE where the C>T alteration occurs. (**B**) Splice products generated by the transfection of the mouse pSmnWT, pSmnC>T or human pSMN1 or pSMNC>T minigene into the HEK 293T cell line were analyzed after RT–PCR and were analyzed using ImageQuant 5.2 showing similar levels of mRNA splicing transcript ratios. (**C**) Sequence results from the 129 Sv/Ev mouse genomic DNA is compared with the results from ENSEMBL showing the absence of a 45 nucleotide repeat in exon 8.

repeat described could be an artifact generated during BAC cloning. To determine whether this sequence was normally present in the mouse genome, we used direct sequencing from high-fidelity PCR-amplified mouse DNA. We found that these 45 nucleotides are absent in the directly sequenced 129 Sv/Ev mouse exon 8 and from the sequence data available on ENSEMBL generated from the C57BL/6 strain (Fig. 1C). Since the 45 nucleotides are absent in the mouse genome and in the minigenes we generated, it is possible that the altered splicing that was previously reported was due to the artificial sequence present in the BAC construct. Our results suggest that the *Smn* gene and the human *SMN1* containing the C>T disruption at position +6 in exon 7 results in a disruption of proper splicing.

Minigenes are regulated by conserved exonic and intronic sequences

To further identify the similarities between the mouse and human *Survival Motor Neuron* regulation, we examined three well-characterized splicing regulatory elements located in exon 7 and intron 7 of both the mouse and human genes. Specifically, we examined the SF2/ASF binding site originally characterized by the Krainer Laboratory (6), the 5′ splice site of exon 7 and the intronic splicing silencer, ISS-N1, located in intron 7, both originally examined by the Singh Laboratory (7,23).

Score matrices derived from the functional binding site consensus sequences of the splicing regulatory protein SF2/ASF have been used to identify ESEs (24). The human *SMN1* genes were originally shown to contain a high-score SF2/ASF motif that is abrogated by the C>T substitution in *SMN2*. Additionally, a second compensatory mutation designed to reconstruct the SF2/ASF ESE in *SMN2* and fully restore exon 7 inclusion was developed using ESEFinder. When the mouse sequence was analyzed using ESEFinder 3.0, the same high scoring SF2/ASF binding site was predicted (values 3.76512 with threshold 1.956). Furthermore, the C>T alteration is predicted to disrupt this site (values 0.81463 with threshold 1.956) similar to the human minigenes (Fig. 2A). By introducing a compensatory A>G point mutation along with the C>T mutation, the predicted SF2/ASF binding site can be restored (values 3.39237 with threshold 1.956). To determine whether correction of the SF2/ASF binding site is sufficient for restoration of full-length transcript, we generated new minigenes containing the compensatory mutation and used in our *in vivo* splicing assay. We found that the A>G correction of the SF2/ASF binding site in both mouse and human restored exon 7 inclusion (Fig. 2A).

To obtain a more direct assessment of the binding of SF2/ASF to the wild-type *Smn* or *Smn* C>T sequence, we per-

Downloaded from https://academic.oup.com/hmg/article/19/21/4239/666050 by guest on 09 April 2024

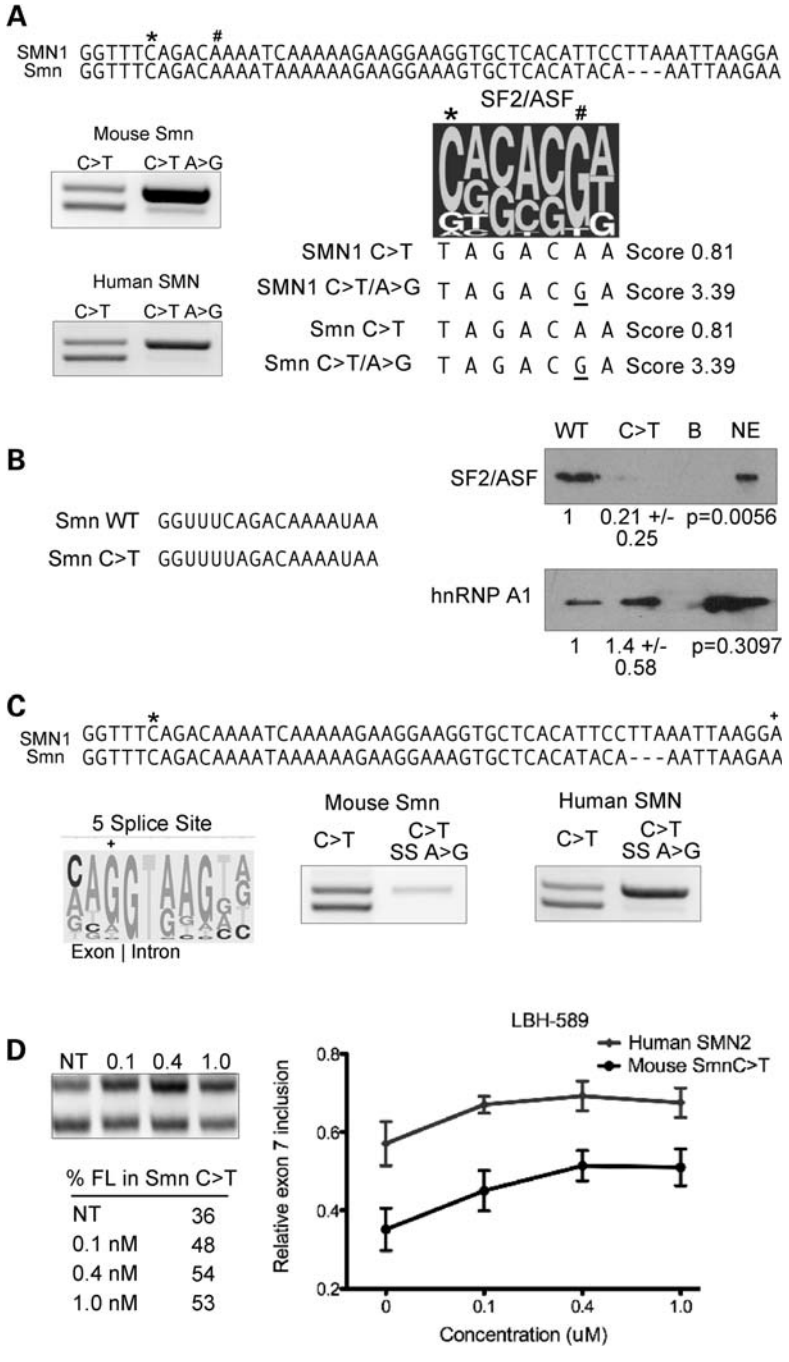

Figure 2. Conserved elements in exon 7 regulate both the mouse and human minigenes. (**A**) Sequence of the human *SMN* and mouse *Smn* exon 7 consensus binding site for SF2/ASF (24). The asterisk represents the exon 7 *SMN2* C>T alteration and the hash symbol the location of the compensatory A>G mutation. The C>T and C>T/A>G binding score generated by ESEFinder 3.0 (21) are given showing that the C>T alteration disrupts the binding site with the A>G mutation restores the score. Splice products generated by the transfection of the mouse pSmn or human pSMN minigene into the HEK 293T show restoration of the full-length transcript in the presence of the compensatory mutation. (**B**) Western blot of proteins recovered from agarose beads covalently linked to the first 17 nucleotides of the wild-type *Smn* or the *Smn* C>T sequenced. Equal molar concentrations of RNA beads were incubated with the HeLa extract in splicing conditions, washed and eluted in SDS sample buffer. Equal amounts were run and probed for SF2/ASF and hnRNP A1. SF2/ASF preferentially bound the wild-type *Smn* RNA, whereas hnRNP A1 preferentially bound the *Smn* C>T RNA. Relative change in binding is measured from three independent experiments using the ImageQuant program. A two-tailed unpaired *t*-test was used to determine the statistical significance. (**C**) Sequence of the human *SMN* and mouse *Smn* exon 7 along with a consensus binding site for the 5′ splice site. The asterisk represents the exon 7 *SMN2* C>T alteration and the plus sign the A>G non-consensus splice site mutation. Splice products generated by the transfection of the mouse or human SMN minigene into the HEK 293T show restoration of the full-length transcript in the presence of the splice site compensatory mutation. (**D**) HEK 293T cells stably transfected with the pSmnC>T minigene were treated with increasing amounts of LBH-589 and harvested 42 h post-treatment. There is an increase in the amount of full-length transcript generated after treatment similar to the increase observed in the endogenous *SMN2* transcripts. All results were confirmed by a minimum of three independent experiments. The 5′ splice site weight matrix was adapted by permission (50) from Macmillan Publishers Ltd: *Nat. Rev. Genet*., **5**(10), 773–782, 2004. The SF2/ASF weight matrix was adapted by permission from (24) Oxford University Press: *Nucleic Acids Res*., **31**(13), 3568–3571, 2003.

Downloaded from https://academic.oup.com/hmg/article/19/21/4239/666050 by guest on 09 April 2024

formed RNA affinity chromatography using the first 17 nucleotides of the wild-type *Smn* sequence or the C>T *Smn* sequence. These sequences were covalently linked to agarose beads and incubated in HeLa cell nuclear extract. Similar to the method published by Cartegni *et al*. (25), SF2/ASF bound to the wild-type *Smn* sequence fragment but had a significant reduction in binding to RNA containing the C>T mutation (Fig. 2B).

These results demonstrate that this SF2/ASF splicing regulatory site in both mouse and human *SMN* is vital for the correct recognition of exon 7. The splicing defect generated by the C>T mutation can be corrected by introducing a compensatory A>G mutation. In addition to the SF2/ASF binding site, the mouse *Smn* containing the C>T point mutation would have all of the sequence elements required to form the *SMN2* exon 7 ESS binding site for Sam68 and, as shown by our blot, hnRNP A1. Indeed, hnRNP A1 bound slightly better to the Smn C>T RNA fragment in our RNA affinity chromatography experiments (Fig. 2B). This conservation again strengthens the similarities observed between the mouse and human genes.

The 5′ splice site is most efficiently recognized when the terminal nucleotide of an exon is a consensus G; however, the human *SMN* genes has a 'weak' exon 7 5′ splice sites as demonstrated by its non-consensus A at the end of exon 7 (Fig. 2C). Using the splice site feature of ESEFinder 3.0, the human *SMN* gene has a predicted suboptimal 5′ splice site (values 5.4646 with threshold 6.67), and by altering the last nucleotide from an A to the consensus G raises the predicted value above threshold (values 8.852). The mouse is also predicted to have a poorly recognized 5′ splice site based on its non-consensus 5′ splice site (Fig. 2C). To examine the effect of the splice site in the minigenes, we used site-directed mutagenesis on the mouse pSmnC>T and human pSMNC>T minigenes, altering the last nucleotide of exon 7 from an A to the consensus G. These minigenes were then used in our *in vivo* splicing assay. We found that the alteration of the 5′ splice site A>G resulted in the correction of splicing with full-length *SMN* transcript being generated even in the presence of the *SMN2* exon 7 C>T alteration in both mouse and human systems (Fig. 2C). Therefore, a 'weak' 5′ splice site is necessary for the C>T disruption to alter pre-mRNA splicing of exon 7 in the *SMN* genes of both the mouse and human.

In addition to the splicing regulatory elements located in exon 7, there are sequences located in intron 7 of the *SMN* genes that affect RNA splicing. One of these elements, ISS-N1, is an intronic splicing silencer (23). This sequence was determined to contain two hnRNP A1 binding sites that are essential for ISS-N1 function (26,27). The original examination of this region indicated that the human and mouse did not share this splicing silencer based on sequence divergence (23). However, no examination in a mouse system was performed. To test the conservation of ISS-N1 between mouse and human, we generated deletions of ISS-N1 in the human and mouse minigenes and analyzed the pre-mRNA splicing products generated. An increase in full-length transcript is observed in both the mouse and human minigenes containing the ISS-N1 deletion, with the mouse showing a 21% increase in full-length transcript, whereas the human minigene showed complete inclusion of exon 7 (Supplementary Material, Fig. S2). The human sequence for ISS-N1 has two hnRNP A1 sites while the mouse *Smn* gene appears to contain only one of these sites (Supplementary Material, Fig. S2a). If hnRNP A1 is indeed responsible of ISS-N1s function in both mouse and human, then this nucleotide divergence, which results in an altered sequence between the two species, could explain why the mouse and human minigenes do not result in identical splicing changes in our minigenes. Both the mouse and human minigenes did show an increase in full-length transcript after deletion of ISS-N1, suggesting that even the introns of the mouse and human gene can contribute to splicing regulation in a similar fashion.

To directly assess the binding of hnRNP A1 to the mouse ISS-N1 sequence, we employed RNA affinity chromatography using the nucleotides that make up the mouse ISS-N1 sequence or the nucleotides that make up the human sequence. These RNAs were covalently linked to agarose beads and incubated in HeLa cell nuclear extract. We found binding of hnRNP A1 to the mouse sequenced, and as expected, this binding was less efficient than the ability of hnRNP A1 to bind the human sequence (Supplementary Material, Fig. S2b).

In addition to the slight difference observed between mouse and human with regard to ISS-N1, we also observed that the level of disruption in the pSmnC>T and pSMNC>T minigenes were less than the levels generated by the pSMN2 minigene, which had an average of 84.9 ± 4.7% skipped transcript (Supplementary Material, Fig. S1a). This suggests that the mouse *Smn* and human *SMN1* gene are similarly regulated, whereas the *SMN2* gene, which is regulated by many of the same factors that control *SMN1* and *Smn* splicing, has additional elements that contribute to increased skipping. Indeed, an *SMN2* intron 7-specific splicing silencer has been previously characterized that contributes to the minor differences in splicing between the pSMNC>T and pSMN2 minigenes (28).

We next asked whether therapeutic compounds that have been shown to affect the splicing of the human *SMN2* transcripts can alter the splicing of the mouse pSmnC>T transcripts further underscoring the regulatory similarities present in the mouse and human *SMN2* gene. LBH-589, an HDAC inhibitor, was shown to increase relative levels of full-length *SMN2* transcript when tested on SMA patient fibroblast cell lines (29). To assess the effectiveness of this drug on the mouse *Smn* gene we generated a HEK 293T cell line stably expressing pSmnC>T and treated it with varying concentrations of LBH-589 that have previously been shown to be effective. Both the mouse pSmnC>T transcripts and the endogenous human *SMN2* transcripts were then amplified and the change in splicing examined. In both the mouse *Smn* and human *SMN2* genes, LBH-589 increased the relative full-length transcript levels with a 16.19% increase in full-length transcript in the pSmnC>T and 11.16% increase in full-length transcript in the *SMN2* gene at 0.4 μM concentrations of LBH-589 (Fig. 2D).

Taken together, these results show that the splicing of both the mouse and human *SMN* exon 7 are regulated by the SF2/ASF ESE, a weak 5′ splice site and the ISS-N1 splicing silencer. Although many splicing elements in the human

Downloaded from https://academic.oup.com/hmg/article/19/21/4239/666050 by guest on 09 April 2024

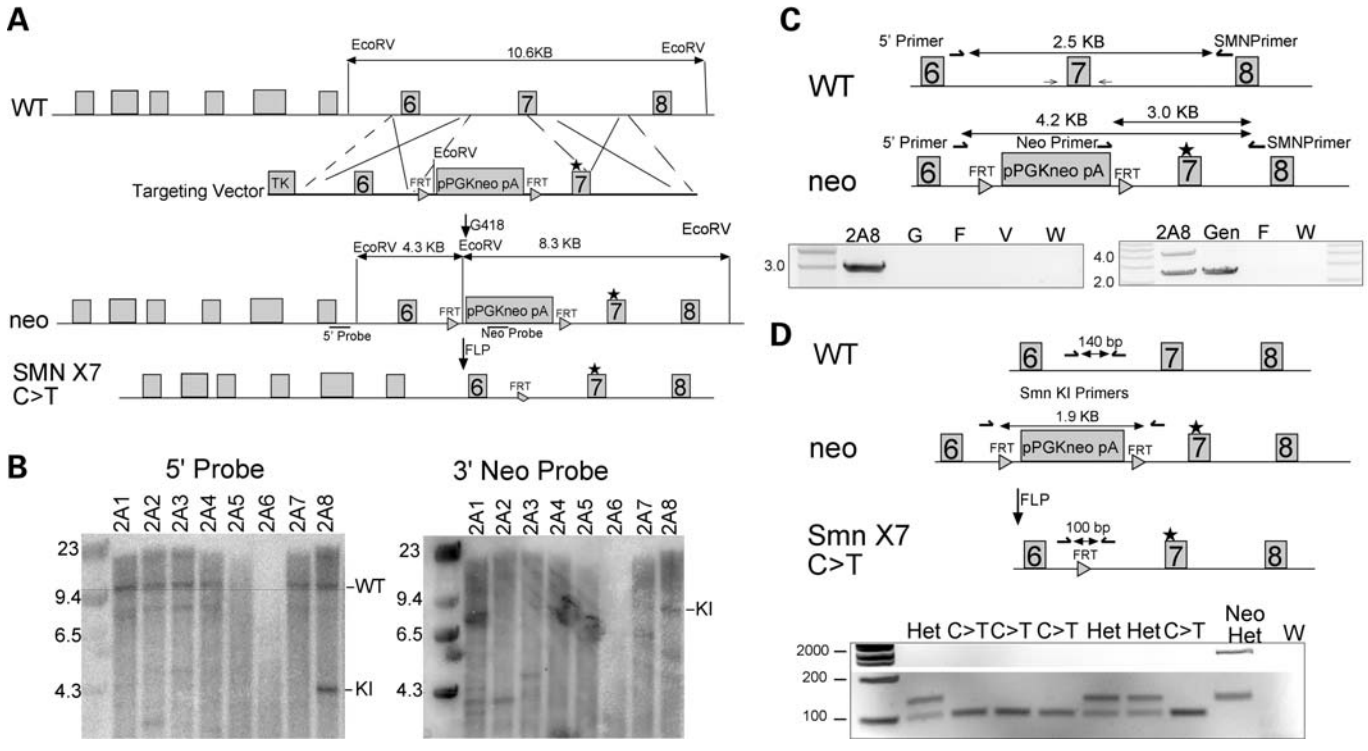

Figure 3. Homologous recombination of the Smn X7C>T mutation into the wild-type mouse *Smn* gene. (**A**) A targeting strategy was devised to insert the *Smn* exon 7 C>T mutation into the mouse *Smn* gene using homologous recombination. (**B**) Correct recombination was confirmed by Southern blot as described previously (49). Using a 5′ probe, the 4.3 kb band present in line 2A8 represents the proper integration of the knock-in allele. A 3′ *Neo* probe also shows the expected 8.3 kb band for line 2A8. (**C**) Recombination of line 2A8 was confirmed by PCR after Southern blot using primers located in the *pPGKneo polyA* and *Smn* gene or in the 5′ arm and the *Smn* gene. Depending on the primer choice, a 3.0 kb band or a 2.4 and 4.2 kb band was amplified, respectively, confirming homologous recombination. (**D**) The resultant mice generated from this ES cell line were crossed to generate germline transmission of our C>T mutation and then crossed with mice expressing FLP recombinase to excise the *Neo* cassette. A PCR in intron 6 flanking the *Neo* cassette and *FRT* sites amplifies either the presence of the *Neo* cassette (1.9 bp) or the removal of the *Neo* cassette (100 bp) in the properly targeted *Smn* C>T allele or a wild-type untargeted band (140 bp).

SMN genes remain to be examined in the mouse context, these results suggest that there is a great degree of shared regulation between the two species. A mouse harboring the C>T point mutation in exon 7 thus may produce slightly more full-length transcript than a mouse containing the *SMN2* transgene based on slight differences observed in our minigene assay. This difference in full-length transcript generated could produce a mouse with a milder phenotype that would live longer and avail therapeutic testing. This mouse would have the benefit of being regulated by the mouse transcriptional machinery and be located in the correct genomic locus making it ideal for testing therapies aimed at splicing correction.

Generation of a knock-in *Smn* C>T mouse

In order to generate the *Smn* exon 7 C>T (X7C>T) mouse model, we generated a targeting vector and mutant mouse as outlined in Materials and Methods. Our final targeting vector contained the mouse exon 7 with the C>T point mutation, a *thymidine kinase* gene for negative selection and a *neomycin* selectable marker (*Neo*) flanked by target sequences for the Flp/FRT recombinase. This allowed for the removal of the *Neo* sequences by Flp recombinase-mediated excision (Fig. 3A). To ensure that the remaining *FRT* sequence would have no effect on the splicing of the *Smn* gene, we generated a mouse pSmnC>T minigene containing the *FRT* sequence located in intron 6. When this minigene was used in our *in vivo* splicing assay, we saw no alteration in the transcripts that were generated (data not shown), suggesting that the *FRT* site in intron 6 will not affect the splicing of the homologously recombined allele.

After ES cell electroporation, the specific targeting event was verified by Southern blot analysis. *Eco*RV digestion of the genomic DNA allowed the detection of the 10.6 kb band present in the wild-type DNA while also allowing the detection of the smaller 4.3 kb transgenic fragment. Additionally, screening the 3′ arm with a probe designed to recognize the *neomycin* cassette detected the expected 8.3 kb band. Of the 288 ES cell lines that we screened, one had the 4.5 and 8.3 kb bands that were generated when homologous recombination occurred (Fig. 3B). We also confirmed recombination by PCR analysis and direct sequencing (Fig. 3C and Supplementary Material, Fig. S3a). The resultant chimeric mice generated from this ES cell line were crossed to generate germline transmission of the X7C>T mutation and then crossed to mice expressing FLP recombinase to excise the *Neo* cassette. Verification of this removal was performed using PCR flanking the *neomycin* cassette (Fig. 3D). Heterozygous *Smn* C>T mice were crossed to generate homozygous

Downloaded from https://academic.oup.com/hmg/article/19/21/4239/666050 by guest on 09 April 2024

Smn C>T mice, which were analyzed for a biochemical and neuromuscular phenotype.

Smn C>T/C>T mice display a splicing defect resulting in lower Smn protein levels

Since SMA is a disease with varying severities ranging from severe pediatric to milder adult onset forms, we examined the mice for symptoms of disease starting at birth and extending into their adult lives. No differences in the Mendelian ratios were detected from the mice generated, suggesting that no pups were reabsorbed due to embryonic lethality (data not shown). Additionally, the *Smn* C>T/C>T mice showed no difference in weight or lifespan when compared with their control littermates (Supplementary Material, Fig. S3b and c). To check that the C>T alteration was disrupting exon 7 inclusion, RNA and protein from these mice was examined to determine whether there was an observable splicing defect. We harvested RNA and protein from the brain, heart, liver, kidney, spleen, spinal cord and skeletal muscle from wild-type, heterozygous and homozygous C>T/C>T mice. The RNA splicing ratio and protein levels were analyzed using RT–PCR and western blots, respectively. RNA from the harvested tissues shows a shift from all full-length transcript in the wild-type mice to skipped transcript in the *Smn* C>T/C>T mice in all tissues analyzed (Fig. 4A and Supplementary Material, Fig. S4a). Additionally, the amount of Smn protein in the SMA mice is decreased when compared with control littermates (Fig. 4B and Supplementary Material, Fig. S4b). Since the mice appeared unaffected in terms of weight and survival but still demonstrated an increase in exon 7 skipping and decrease in protein, this we continued to look for a mild, late-onset SMA phenotype.

Phenotypic analysis of the *Smn* C>T/C>T mice

In SMA patients, loss of motor neurons leads to denervation and atrophy of muscle. To examine both the spinal cord and skeletal muscle for denervation and atrophy, the tissues were harvested and cross-sections stained and analyzed. The spinal cord morphology was examined in the mice and had no evidence of severe denervation or gross morphological abnormalities detectable compared with littermates (Supplementary Material, Fig. S5). This observation is consistent with observations made in individuals with a mild phenotype that had relatively preserved lower motor neurons populations when compared with SMA type 1 cases (30). Additionally, the gastrocnemius and quadriceps of the mice were hematoxylin and eosin (H&E) and succinic dehydrogenase (SDH) stained and examined for evidence of muscular atrophy and alteration in fiber type based on fiber size and morphology. Fiber type was unchanged in the tissues examined. However, transverse sections of the muscle revealed an increase in larger-sized fibers in *Smn* C>T/C>T animals ($n = 2$ controls and $n = 2$ *Smn* C>T/C>T) examined at 60 days of age and mice ($n = 3$ control and $n = 3$ *Smn* C>T/C>T) examined at 6 months of age, resulting in a slightly larger average fiber size due to a shift to larger muscle fibers when compared with age-matched controls (Fig. 5). This is indicative of a phenotype that has been observed in some Kugelberg–Welander SMA patients as well as in mild animal models of SMA (31–33).

To better characterize these mice and determine whether they display other more subtle symptoms of the SMA phenotype, we examined some of their behavioral traits. Motor activity, rearing and grip strength were all measured in the SMA mice beginning at 30 days after birth. To access motor activity and rearing, mice were put in a photobeam activity system and their activity and rearing was measured. SMA mice showed a significant decrease ($P < 0.05$) in the amount of movement when compared with their control littermates (average activity of 2253 line breaks in the control group and 1534 line breaks in the *Smn* C>T/C>T) and were less likely to rear on to their hind limbs (average rearing of 95 times in the control group and 34 times in the *Smn* C>T/C>T) (Fig. 6B). This decrease in activity was observed throughout their lives starting at 60 days of age (Fig. 6C). Additionally, grip strength was measured with hind limb strength being significantly different from the control mice ($P < 0.05$) (Fig. 6A). This is consistent with the symptoms observed in adult-onset SMA where the legs are often first and most affected while the arms remain normal (34,35). Activity, hindlimb grip strength and rearing are known to be decreased in the severe models of SMA and SMA patients (18,34,36). Thus, this decrease in activity and decrease in grip strength are consistent with a mild form of SMA and correlate with the mild hypertrophy in muscle fiber size observed in our *Smn* C>T/C>T mice.

Examining neuromuscular transmission in our adult-onset SMA mouse

In an attempt to further decrease the levels of Smn protein and possibly increase the severity of the SMA disease phenotype, the *Smn* C>T/C>T mouse was crossed to the previously generated mouse containing a knock-out mutation in the *Smn* allele (*Smn*+/−) (10). This mouse contains a targeted mutant *Smn* allele that effectively inactivates the *Smn* gene product. It is expected that the lower levels of Smn protein would increase neuromuscular defects in the *Smn* C>T/- mice. This *Smn* C>T/- mouse also exhibits decreased grip strength and activity along with lower Smn protein levels (Supplementary Material, Fig. S6a). We used the *Smn* C>T/- mouse to examine synaptic transmission in the tibialis anterior muscle. It has previously been found that the number of vesicles released (quantal content) at the neuromuscular junction (NMJ) is reduced in SMA mice (37). We recorded endplate currents and spontaneous miniature endplate currents as described previously (37). We found no differences in neuromuscular transmission in the TA muscle from the *Smn* C>T/- mice when compared with control animals (Supplementary Material, Fig. S6b). Although the TA has shown reduced quantal content when examined in the severe SMA mice, this distal muscle may have a milder phenotype than more proximal muscles so it remains possible that we missed defects in quantal content present in proximal muscles.

Finally, the NMJ was examined for evidence of axonal sprouting in the transversus abdominis muscle and gastrocnemius muscles. Recent studies in SMA models have also shown morphological abnormalities of NMJ synapses (18,37). Axonal sprouting can compensate for denervation in motor neuron diseases and has been observed in some, but not all,

Downloaded from https://academic.oup.com/hmg/article/19/21/4239/666050 by guest on 09 April 2024

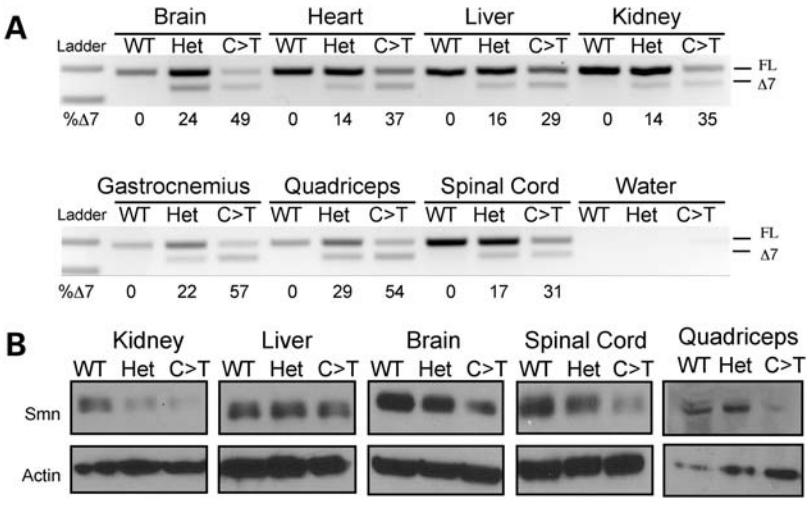

Figure 4. Splicing and protein levels from mouse *Smn* C>T gene are disrupted. (**A**) RT–PCR was performed on RNA from snap-frozen homogenized mouse tissue from the brain, heart, liver, kidney, gastrocnemius, quadriceps and spinal cord. The skipped isoform was increasingly present in the mice containing the exon 7 C>T allele in all tissues analyzed. Quantification was carried out using densitometry using the ImageQuant program. (**B**) Western blot analysis from tissues of *Smn* C>T/C>T mice (anti-SMN, 1:3000 dilution; BD Bioscience). The blot was subsequently stripped and hybridized with a beta-actin (1:1000 dilution; Sigma) to control for loading. Levels of Smn protein were decreased in the mice containing the exon 7 C>T allele. WT = WT/WT, Het = WT/C>T and C>T = C>T/C>T.

SMA mouse models (38,39). To determine the extent of sprouting, synapses in these muscles from mild SMA mice were examined. We found no evidence of sprouting in the animals examined (Supplementary Material, Fig. S6c). Thus, the Smn C>T/- mice show behavioral deficits indicative of the SMA phenotype, even in the absence of detectable NMJ defects.

In summary, we have used comparative genomics to analyze the *SMN* genes of both mouse and human to show a high level of similarity between the splicing regulation of the mouse *Smn* and the human *SMN* genes. By engineering the *SMN2* C>T alteration into the mouse *Smn* gene using homologous recombination, we have developed a new mouse model of SMA. This model has *Smn* splicing defects that lead to decreased Smn protein levels alterations in muscle morphology and decreases in activity and rearing.

DISCUSSION

The human genome harbors two copies of the essential gene, *Survival Motor Neuron. SMN1* mRNA expresses full-length transcript, whereas *SMN2* produces only low levels of full-length transcript. The critical difference between *SMN1* and *SMN2* is a silent nucleotide transition in *SMN* exon 7 (2,40). Using comparative genomics, comparing the genes from mouse and human can provide a better understanding of the function of conserved genes and, additionally, how species have evolved and a gene changed. Indeed, by using this approach, we were able to show that both the mouse and human *SMN* genes were regulated by the conserved exon 7 ESE, a suboptimal 5′ splice site and the intronic element ISS-N1. Analysis using and comparing the results from multiple minigene experiments allows an even deeper level of understanding of how a gene like the human *SMN2* is regulated and which elements have been evolutionarily conserved.

It was our hypothesis that using the intermediate splicing level generated by the mouse pSmnC>T point mutation when compared with the pSMN2 minigene, it would be possible to generate a mouse that would live longer and be more amenable to testing new therapies for SMA. When the C>T alteration was engineered into the mouse *Smn* gene, the amount of full-length Smn protein is decreased and leads to a mouse with a very mild SMA phenotype. This mouse is a good model for adult-onset SMA (type III or IV). Though the mild phenotype of our mice could be due to differences in the regulation of the mouse and human *SMN* genes, it is also possible that mice may not be as sensitive to decreased SMN levels and that a difference in the threshold between mouse and human could also account for the differences in disease severity. Perhaps due to the difference in size, morphology or molecular make-up of the alpha-motor neurons, the mouse requires a more substantial loss of Smn protein before severe pediatric symptoms arise.

Analysis of the type II SMA Delta7 mouse models found that the testes had a higher level of full-length transcript being generated than any other tissue examined (41). Likewise, splicing ratios generated in various tissues in the *Smn* C>T/C>T mouse varied from tissue to tissue, suggesting that there may be tissue-specific splicing regulation of the *Smn* gene. These differences seen in the *Smn* C>T/C>T mice and the existence of an already identified factor binding in the testes of the SMA Delta7 mice suggest that the *SMN* genes may be regulated in a tissue-specific manner. Such tissue-specific regulation could explain why the motor neurons are more sensitive to decreased SMN levels and are the cell type lost in SMA. Perhaps the motor neurons regulate exon 7 splicing of the *SMN* genes in a unique way. Thus, the *Smn* C>T/C>T mouse provides a tool that will allow us to better elucidate any tissue-specific function in the alternative splicing of the *SMN* genes.

Downloaded from https://academic.oup.com/hmg/article/19/21/4239/666050 by guest on 09 April 2024

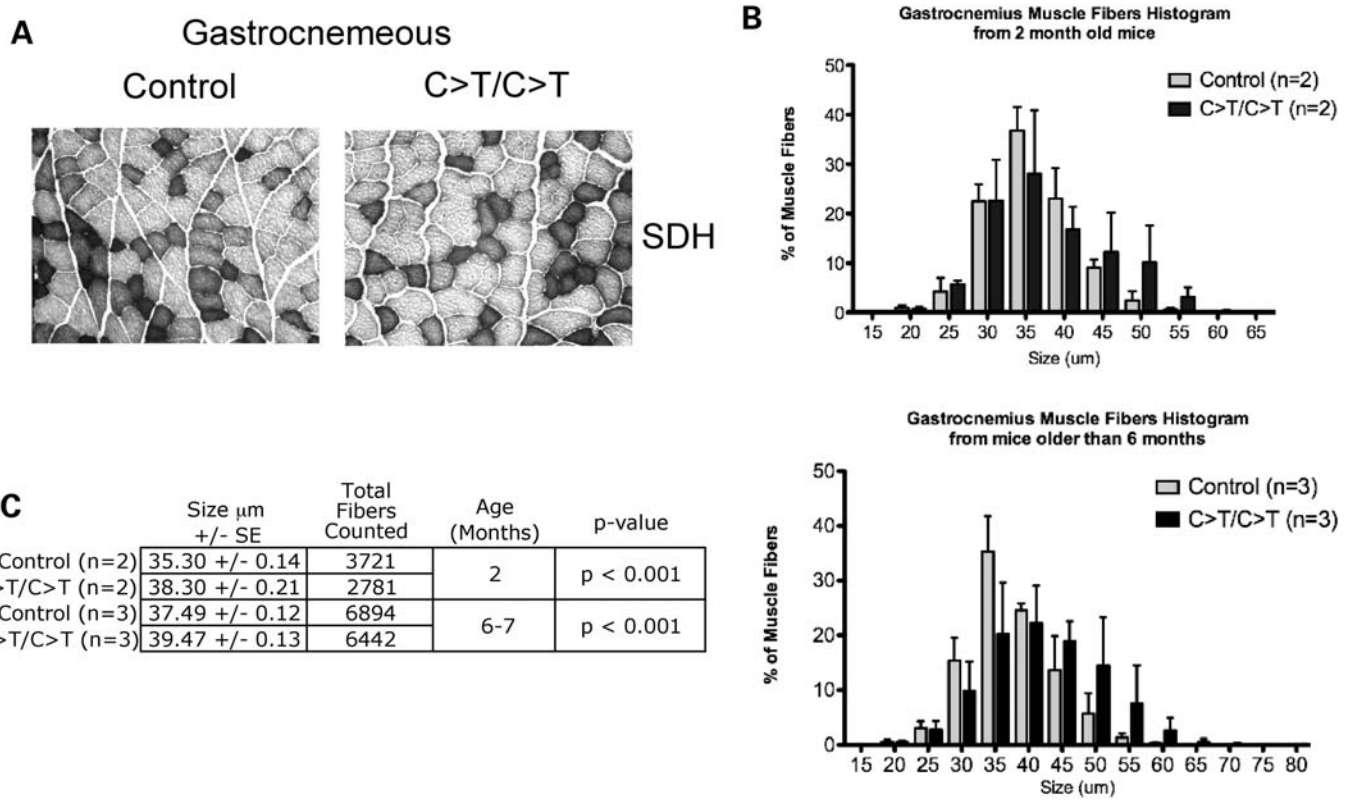

C

	Size μm +/- SE	Total Fibers Counted	Age (Months)	p-value
Control (n=2)	35.30 +/- 0.14	3721	2	p < 0.001
C>T/C>T (n=2)	38.30 +/- 0.21	2781		
Control (n=3)	37.49 +/- 0.12	6894	6-7	p < 0.001
C>T/C>T (n=3)	39.47 +/- 0.13	6442		

Figure 5. Histological examination of *Smn* C>T/C>T mice skeletal muscle shows increased incidence of larger muscle fibers. (**A**) Skeletal muscle was examined for evidence of phenotype associated with SMA at 20× magnification. Fiber types based on SDH staining showed no differences between the *Smn* C>T/C>T and control animal changes. (**B**) Measurements from 2-month-old gastrocnemius muscle fiber sizes show an increase in the number of larger fibers in the *Smn* C>T/C>T when compared with control animals resulting in a slightly larger average muscle fiber size. Similar changes were observed in animals examined at 6 months of age. (**C**) Table showing the changes in average muscle size from the gastrocnemius muscle from the 2- and 6-month-old mice. The average size was statistically significant when analyzed using a two-tailed *t*-test.

The *Smn* C>T/C>T mouse additionally offers us the opportunity to examine new modifiers of the *Smn* gene. By crossing these mice to mice with other genetic modifications, the role other genes play in the severity of the SMA phenotype can be assessed. As the majority of the current mouse models are so severe that death occurs within the first 2 weeks of life, assaying genes that have a detrimental effect on RNA splicing or phenotype can become challenging, if not impossible. The mild SMA model that we have generated, which appears to be teetering between a normal and disease phenotype, is uniquely suited to assess these potential modifying genes such as *NAIP*, *H4F5* and *Tra2β* (*Sfrs10*) (42–44) or as-yet unidentified modifiers of the SMA disease and *SMN2* splicing.

Tra2β (*Sfrs10*) is an especially exciting gene to examine as a knock-out mouse has recently been generated and examined with respect to the splicing of the wild-type *Smn* (45). Although complete knock-out of *Tra2β* was embryonic lethal, in the heterozygous condition (*Tra2β*+/−) mice were viable. When the endogenous *Smn* gene was examined in the *Tra2β*+/− mouse, there was a mild increase in exon 7 skipping. Since Tra2βis a known splicing regulator of *SMN*, a mouse carrying the *Smn* C>T alleles and expressing *Tra2β* in the heterozygous condition could yield an increase in exon 7 skipping and a more severe SMA like phenotype. This is just one example of a potential modifier of both *SMN* splicing and the SMA phenotype that could be examined in our *Smn* C>T/C>T mice. Similar experiments could be undertaken with other potential modifiers of SMA or *SMN2* splicing.

Additionally, new modifiers can be identified by crossing the *Smn* C>T mouse onto different genetic backgrounds and monitoring the disease phenotype. Backgrounds that increase the phenotypic severity can then be analyzed to identify the causative genetic changes. The work reported here was performed on mice from a mixed 129 Sv/Ev–C57BL/6 background. By breeding the mice onto a congenic background, variations in disease phenotype can be assessed to identify the possible modifier of the SMA phenotype. Understanding how other genes affect the SMA disease phenotype could provide unique points of therapeutic intervention and bring a greater understanding of SMA.

The completion of this research has provided a better understanding between the *SMN* genes of mice and humans and gives insight into conserved elements within the genes that could potentially be targeted to correct exon 7 splicing. Additionally, by generating the mouse knock-in model, we have a better understanding of how the *Smn* gene in mice is regulated, giving insight into the amount of Smn protein and transcript ratios that are required to produce the SMA phenotype.

Downloaded from https://academic.oup.com/hmg/article/19/21/4239/666050 by guest on 09 April 2024

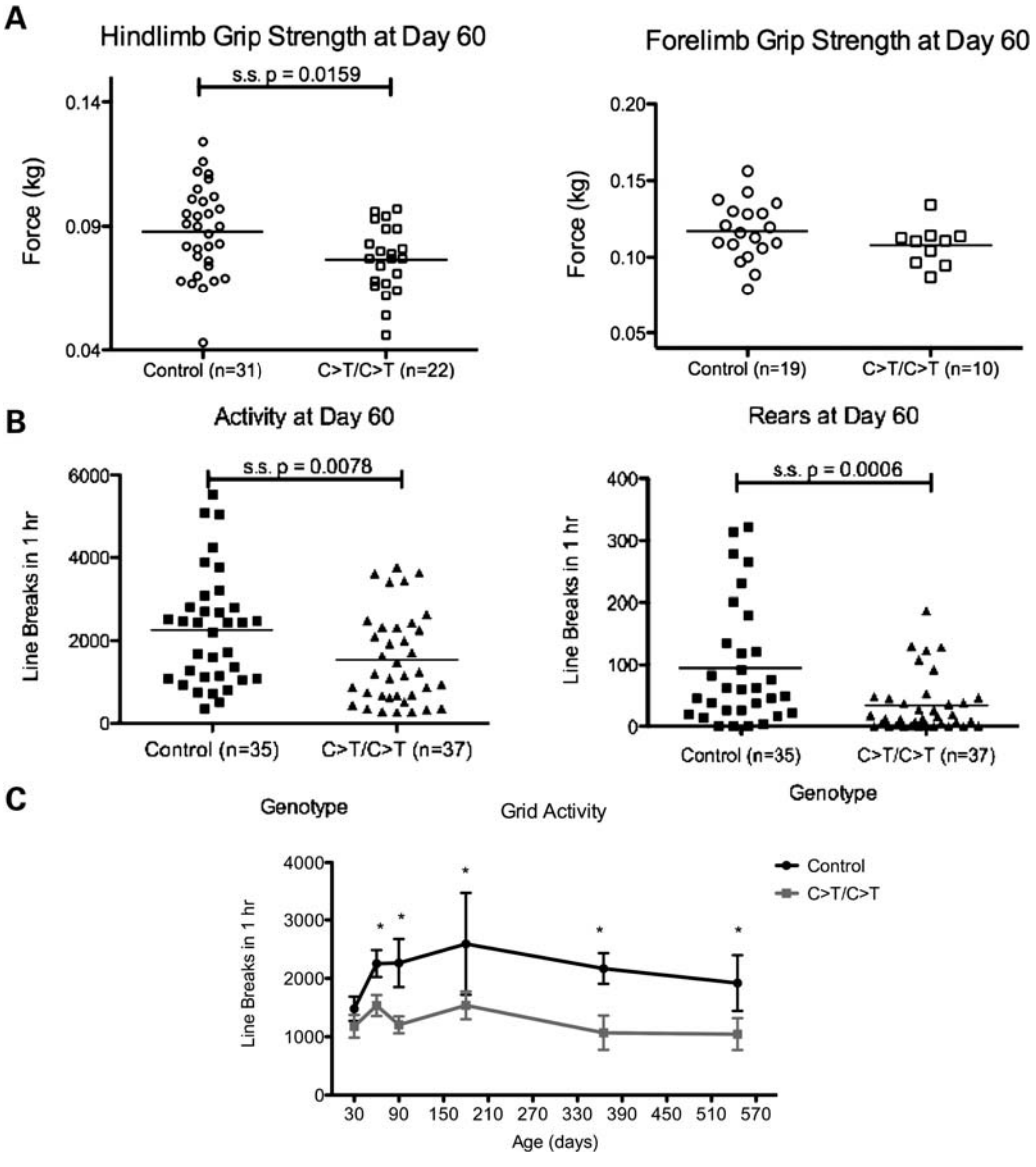

Figure 6. Behavioral analysis reveals the activity and strength deficits in *Smn* C>T/C>T mice. (**A**) Plot of limb grip strength for the *Smn* C>T/C>T mice. A line displays mean values with each point representing a different mouse. A significant decrease in hindlimb grip strength but not forelimb grip strength is observed between the *Smn* C>T/C>T mice and control littermates. (**B**) Graph of locomotive activity for the *Smn* C>T/C>T mice. A significant decrease in rearing and locomotion was observed starting at 60 days between the *Smn* C>T/C>T mice and control littermates. (**C**) The decrease in activity is significant throughout the lives of the *Smn* C>T/C>T mice.

To find a promising treatment for SMA, it is necessary to understand the dynamic interactions involved in the regulation of the *SMN* RNA and have models available that allow rigorous testing of new drug therapies. Unfortunately, the very mild phenotype of the *Smn* C>T/C>T mice makes measuring functional rescue of the SMA phenotype difficult. However, the extended lifespan of our mice allows the treatment of the disease at later developmental time points, beyond which other SMA mouse models do not survive. Additionally, crossing the *Smn* C>T/C>T with any of the currently available *SMN2/SMN2* containing models could generate a mouse that could be used to gain more information on a compound's therapeutic effect. The *Smn* C>T/C>T; *SMN2*/*SMN2* mouse would have the benefits of containing both the mouse *Smn* C>T and human *SMN2* gene present, both containing their endogenous promoter. Additionally, the mouse *Smn* C>T gene would be in its correct genomic context. Compounds tested in the *Smn* C>T/C>T; *SMN2/SMN2* mouse would allow the analysis of both *SMN* genes to get a better understanding of the effect of the drug on *SMN* splicing. A compound that affects splicing of only one gene may be acting through a non-conserved element, whereas changes in splicing of both genes would represent a compound acting on a conserved element. As animal testing represents an investment in both time and resources, being able to monitor an additional *Smn* gene and potentially better understand the mechanism of a new drug therapy is an excellent resource.

Downloaded from https://academic.oup.com/hmg/article/19/21/4239/666050 by guest on 09 April 2024

Development of the *Smn* C>T/C>T mouse provides a new and useful model organism of SMA and lends a deeper understanding of the *Survival Motor Neuron* gene and how the *SMN* gene is regulated in both mice and humans. The new *Smn* C>T/C>T SMA mouse model has the *Smn* gene regulated by natural epigenetic and transcriptional mechanisms and produces lower levels of Smn protein due to an increase in exon 7 skipping. The *Smn* C>T/C>T mouse can thus be of use in understanding the role of SMN protein in SMA and teasing apart the complex RNA regulation that is involved in the *SMN* genes. Furthermore, this new model for the Kugelberg–Welander disease can additionally be used for the identification of modifiers of the SMA phenotypes and to test new therapies for SMA aimed at correction of *SMN2* splicing.

MATERIALS AND METHODS

Generation of splicing competent minigenes

The pSMN1 and pSMNC>T minigenes were constructed previously (46). The minigene pSMN2 was generated by PCR amplification using high-fidelity *taq* polymerase (Roche, Indianapolis, IN, USA) and hSMN X6FW primer (5′-ataattccccccaccacctc-3′) and hSMN X8RV primer (5′-cacatacgcctcacataca-3′), cloned in Invitrogen's (Carlsbad, CA, USA) TOPO TA cloing vector, verified by direct sequencing and subcloned into Stratagene's (La Jolla, CA, USA) CMV-2B vector. Similarly, the mouse pSmnWT minigene was constructed to contain the wild-type mouse genomic *Smn* fragment containing exons 6–8 and their corresponding intronic sequences using primer (5′-ttcggatccataatcccgcca ccccctcccatctc-3′) and primer (5′-accgaattccgactgggtagactg ccttccgacacg-3′), cloned into Invitrogen's TOPO TA vector and subcloned into Stratagene's CMV-2B vector. Site-directed mutagenesis was then performed to convert the exon 7 C>T using QuikChange XL Site Directed Mutagenesis Kit (Stratagene) to generate the pSmnC>T minigene. Mutations in the SF2/ASF, 5′ splice site and deletion of ISS-N1 were generated used QuikChange XL Site Directed Mutagenesis Kit (Stratagene). All Mutagenesis primers are listed in Supplementary Material, Table S1.

Cell culture

Unless otherwise stated, all tissue culture media and supplements were purchased from Invitrogen. Human embryonic kidney 293 (HEK-293T) cells (American Type Culture Collection, Manassas, VA, USA) non-small cell lung carcinoma (H1299) cells (American Type Culture Collection), mouse myoblast (C2C12) cells (American Type Culture Collection), human breast cancer (MCF7) cells (American Type Culture Collection) and human (HeLa) cells (American Type Culture Collection) were cultured in Dulbecco's modified Eagle's medium supplemented with 10% fetal bovine serum, 100 U/ml penicillin and 100 μg/ml streptomycin.

Comparison of the mouse exon 8 sequence

Mouse exon 8 was sequenced from genomic 129 Sv/Ev DNA and compared with the sequences available on ENSEMBL from the C57/BL6 strain (ENSMUST00000022147) with alignment done using the DNASTAR Lasergene SeqMan Pro version 8.0.2 (16) program.

Transfection and *in vivo* splicing assays

All reagents were used according to the manufacturer's recommendations. Transient transfections of cells with 2 μg plasmid DNA were performed with 6 μl Fugene 6 (Roche). Cells were transfected and RNA harvested as described previously (46). Total RNA was harvested from mouse tissues using RNAeasy Mini Kit (Qiagen, Valencia, CA, USA). To generate cDNA from mouse tissue, reverse transcription was carried out with Transcriptor Reverse Transcriptase (Roche) using a random primer $p(dN)_6$. Generally, 1.0–2.0 μg of total RNA was used per 20 μl of the reaction mixture. Minigene-specific spliced products were subsequently amplified with *Taq* polymerase (Sigma, St Louis, MO, USA) and the following primer combinations with sequence provided in Suplementary Material, Table S2: FLAG and hSMN X8as1 for human pSMN and FLAG and mSmnX8as1 for the mouse pSmn. Mouse tissue-spliced products were amplified with *Taq* polymerase and the following primer combinations with sequence provided in Supplementary Material, Table S2: mSmn X6 1F and mSmnX8as1 for the mouse *Smn*. Human SMN1/SMN2 endogenous products were amplified with hSMN X6s3 and hSMN X8as1. Analysis and quantifications of spliced products were performed using ImageQuant 5.2 (GE Healthcare Live Sciences, Piscataway, NJ, USA). Results were confirmed by a minimum of three independent experiments.

RNA affinity chromatography

WT (GGUUUCAGACAAAAUAA), C>T (GGUUUUAGAC AAAAUAA), hISS-N1 (CCAGCAUUAUGAAAGU) and mISS-N1 (UCAUUUUAAAAGC) RNA was generated by Dharmacon (Lafayette, CO, USA). Five nanomoles of RNA was suspended in a 400 ml reaction mixture containing 100 mM sodium acetate pH 5.0 and 5 mM sodium m-periodate (Sigma) for 1 h in the dark at room temperature. After ethanol precipitation, the RNA was resuspended in 50 μl of 0.1 M sodium acetate pH 5.0. A 200 μl aliquot of adipic acid dihydrazide agarose bead 50% slurry (Sigma) was washed four times in 5 ml of 0.1 M sodium acetate pH 5.0 and pelleted after each wash at 100*g* for 3 min in a clinical centrifuge. After final wash, the beads were resuspended in 150 μl of 0.1 M sodium acetate pH 5.0. Fifty microliters of RNA was mixed with the 150 μl of beads and rotated at 4°C overnight, then pelleted and washed three times in 1 ml of 2 M NaCl and then three times in 1 ml of buffer D (20 mM HEPES-KOH pH 8.0, 20% glycerol, 0.1 M KCl, 0.2 mM EDTA, 0.5 mM DTT) and resuspend in 125 μl of buffer D. A 300 μl *in vitro* splicing reaction mixture was made containing 120 μl of the nuclear extract and 125 μl of the RNA bound beads. The reaction was incubated at 30°C for 40 min gently mixing every 5–10 min, then the protein-bound RNA/beads were washed three times in buffer D with 150 mM KCl. The beads were resuspended in 50 μL 2× SDS buffer, heated at 100°C for 5 min quickly, spun down, collected and run on a 10%

Downloaded from https://academic.oup.com/hmg/article/19/21/4239/666050 by guest on 09 April 2024

SDS–PAGE Gel. Blots were probed using anti-SF2/ASF (1:500 dilution; Zymed) and anti-hnRNPA1 (1:200 dilution; Abcam).

Generation of knock-in mice, breeding strategy and genotyping

To generate the *Smn* Exon 7 C>T (X7C>T) mutant mouse, we used standard recombinant mouse ES cell techniques and a targeting strategy outlined in Manipulation the Mouse Embryo (47). The 5′ and 3′ homologous arms of the targeting vector were cloned from the mouse genome at the *Smn* locus and then subcloned into the pLG1 vector (obtained from Richard Behringer). These regions of homology were cloned from genomic DNA originating from the same mouse strain (129 Sv/Ev) as the ES cells. After the sequences were confirmed, the 3′ homologous arm was mutagenized to include the human C>T exon 7 alteration found in the *SMN2* gene. ES cells were electroporated by the Nationwide Children's Research Institute's Transgenic and Embryonic Stem Cell Core using the purified and linearized targeting vector. Two hundred and eighty-eight resistant ES colonies grown in a medium containing G418 and Ganciclovir were selected to screen for homologous recombination. ES cell genomic DNA was digested with *Eco*RV (New England Biolabs, Ipswich, MA, USA) and probed by Southern blot analysis using probes located in the 5′ and 3′ arms. The correctly targeted ES cell line was again confirmed by PCR using primers located in the *pPGKneo pA* and *Smn* gene or in the 5′ arm and the *Smn* gene. The C>T knock-in mutation was detected by PCR using the primer mSmn X7 Chk and primer mSmn X7 R with sequence and conditions in Supplementary Material, Table S2. The 383 bp fragment was then digested with *Hpy*188I (New England Biolabs). After digesting, the wild-type *Smn* generated two bands at 267 and 116 bp whereas the C>T remains undigested. Direct sequencing from PCR product used mSmn X7 Chk F primer to confirm the C>T mutation.

The resultant mice generated from this ES cell line were crossed to generate germline transmission of the C>T mutation and then crossed with mice expressing FLP recombinase (Jackson Laboratories #003946) to excise the *Neo* cassette. PCR using Smn KITEST S2 and Smn KITEST AS2 detected the removal of the *Neo* cassette with conditions and sequence information provided in Supplementary Material, Table S2. Heterozygous *Smn* C>T mice lacking the *Neo* cassette were intercrossed and analyzed for neuromuscular phenotype. *Smn* C>T/- mice were generated by crossing mice containing the mouse *Smn* knock-out allele to the *Smn* C>T/C>T mice. *Smn* knock-out allele was detected by PCR as described previously (10). The *Smn* C>T/C>T mice were all on an F3 C57BL/6 background (mice generated from ES cells of a 129 Sv/Ev background were backcrossed three times with C57BL/6 mice) with the *Smn* C>T/- mice on an F4 background. Mice were only compared with control littermates from within the same background to prevent the potential for mixed background effect to influence results. All animal procedures were approved by Nationwide Children's Hospital Institutional Animal Care and Use Committee.

Western blot analysis

Mouse tissue was ground up using a mortar and pestle in liquid nitrogen and homogenized in RIPA buffer using a Tissumizer (Teledyne Tekmar, Cincinnati, OH, USA). Protein was quantified and equal amounts loaded on a 12% polyacrylamide gel. Blots were probed using anti-actin (1:1000 dilution; Sigma), anti-SMN (1:3000 dilution; BD Bioscience, San Jose, CA, USA), and anti-beta-tubulin (1:50 dilution, The Developmental Studies Hybridoma Bank, Iowa City, IA, USA) antibodies according to the manufacture's recommendations.

Histology and muscle morphology

Skeletal muscles were dissected from mice at either 2 or 6–7 months of age and snap-frozen in liquid nitrogen-cooled isopentane. Cryosections, 12–20 μm thick, were stained with either H&E or SDH staining as described previously (48). Sections were photographed in a brightfield microscope at 10× magnification. Three fields of view were sampled from control and *Smn* C>T/C>T gastrocnemius muscle sections. Microscope software Axiovision 4.7 was used to measure and record muscle fiber diameters in micrometers. Two-tailed *t*-test was performed using GraphPad Prism 5.0b to determine statistical significance in fiber size.

Weight, locomotion activity, rearing and grip strength

Each mouse was weighed at days 60 and 365 with results recorded in grams. Two-tailed *t*-test was performed using GraphPad Prism 5.0b to determine statistical significance. To measure activity and rearing, each mouse was placed in the center of a 16 inch × 16 inch SD Instruments PAS Photobeam Openfiled Activity System (San Diego Instruments, San Diego, CA, USA) and allowed to explore the box for 5 min. After 5 min, the computer begins to measures the number of times the mouse enters a new grid or reared onto their hind limbs. Control animal (WT/WT and WT/C>T) were compared with SMA animals (C>T/C>T) at ages 30, 60, 90, 180, 365 and 545 days. One-tailed *t*-test was performed using GraphPad Prism 5.0b to determine statistical significance.

Grip strength was assessed using a Chatillon Digital Force Gage Grip Strength Meter (Columbus Instruments, Columbus, OH, USA). Grip strength meter testing was performed by allowing the animals to grasp a platform with hind limbs or forelimbs, followed by pulling the animal until it released the platform with the force measurement recorded in three separate trials. One-tailed *t*-test was performed using GraphPad Prism 5.0b to determine statistical significance.

SUPPLEMENTARY MATERIAL

Supplementary Material is available at *HMG* online.

ACKNOWLEDGEMENTS

We thank Steven Mapel, Lisa Caldwell, Dr Cathy Lutz, Vicki McGovern from Dr Arthur Burghes's Laboratory and Kevin Foust from Dr Brian Kaspar's Laboratory for the generous assistance they provided. We would also like to thank two

Downloaded from https://academic.oup.com/hmg/article/19/21/4239/666050 by guest on 09 April 2024

anonymous reviewers for their helpful comments that led to an improved manuscript.

Conflict of Interest statement. Neither this manuscript nor any similar manuscript, in whole or in part, other than an abstract, has been or will be submitted to or published in any other scientific journal by the named authors. All authors are aware of and agree to the content of the paper and their being listed as authors on the paper. There are no financial or other interests with regard to the submitted manuscript that might be construed as a conflict of interest.

FUNDING

This work was supported by The Research Institute at Nationwide Children's Hospital, the National Institute of Neurological Disorders and Stroke (NINDS) Grant (1R21NS054690 to D.S.C.), the National Institute of General Medical Sciences (NIGMS) Grant (1F31GM080151-01A1 to J.T.G.) and the National Institute of Neurological Disorders and Stroke (NINDS) Grant (P01NS057228 to M.M.R.).

REFERENCES

1. Pearn, J. (1978) Incidence, prevalence, and gene frequency studies of chronic childhood spinal muscular atrophy. *J. Med. Genet.*, **15**, 409–413.
2. Lefebvre, S., Burglen, L., Reboullet, S., Clermont, O., Burlet, P., Viollet, L., Benichou, B., Cruaud, C., Millasseau, P., Zeviani, M. *et al.* (1995) Identification and characterization of a spinal muscular atrophy-determining gene. *Cell*, **80**, 155–165.
3. Lorson, C.L., Hahnen, E., Androphy, E.J. and Wirth, B. (1999) A single nucleotide in the SMN gene regulates splicing and is responsible for spinal muscular atrophy. *Proc. Natl Acad. Sci. USA*, **96**, 6307–6311.
4. Monani, U.R., Lorson, C.L., Parsons, D.W., Prior, T.W., Androphy, E.J., Burghes, A.H. and McPherson, J.D. (1999) A single nucleotide difference that alters splicing patterns distinguishes the SMA gene *SMN1* from the copy gene *SMN2*. *Hum. Mol. Genet.*, **8**, 1177–1183.
5. Kashima, T. and Manley, J.L. (2003) A negative element in SMN2 exon 7 inhibits splicing in spinal muscular atrophy. *Nat. Genet.*, **34**, 460–463.
6. Cartegni, L. and Krainer, A.R. (2002) Disruption of an SF2/ASF-dependent exonic splicing enhancer in SMN2 causes spinal muscular atrophy in the absence of SMN1. *Nat. Genet.*, **30**, 377–384.
7. Singh, N.N., Androphy, E.J. and Singh, R.N. (2004) *In vivo* selection reveals combinatorial controls that define a critical exon in the spinal muscular atrophy genes. *RNA*, **10**, 1291–1305.
8. Lefebvre, S., Burlet, P., Liu, Q., Bertrandy, S., Clermont, O., Munnich, A., Dreyfuss, G. and Melki, J. (1997) Correlation between severity and SMN protein level in spinal muscular atrophy. *Nat. Genet.*, **16**, 265–269.
9. Coovert, D.D., Le, T.T., McAndrew, P.E., Strasswimmer, J., Crawford, T.O., Mendell, J.R., Coulson, S.E., Androphy, E.J., Prior, T.W. and Burghes, A.H. (1997) The survival motor neuron protein in spinal muscular atrophy. *Hum. Mol. Genet.*, **6**, 1205–1214.
10. Schrank, B., Gotz, R., Gunnersen, J.M., Ure, J.M., Toyka, K.V., Smith, A.G. and Sendtner, M. (1997) Inactivation of the survival motor neuron gene, a candidate gene for human spinal muscular atrophy, leads to massive cell death in early mouse embryos. *Proc. Natl Acad. Sci. USA*, **94**, 9920–9925.
11. Monani, U.R., Sendtner, M., Coovert, D.D., Parsons, D.W., Andreassi, C., Le, T.T., Jablonka, S., Schrank, B., Rossol, W., Prior, T.W. *et al.* (2000) The human centromeric survival motor neuron gene (SMN2) rescues embryonic lethality in Smn(−/−) mice and results in a mouse with spinal muscular atrophy. *Hum. Mol. Genet.*, **9**, 333–339.
12. DiDonato, C.J., Chen, X.N., Noya, D., Korenberg, J.R., Nadeau, J.H. and Simard, L.R. (1997) Cloning, characterization, and copy number of the murine survival motor neuron gene: homolog of the spinal muscular atrophy-determining gene. *Genome Res.*, **7**, 339–352.
13. DiDonato, C.J., Brun, T. and Simard, L.R. (1999) Complete nucleotide sequence, genomic organization, and promoter analysis of the murine survival motor neuron gene (*Smn*). *Mamm. Genome*, **10**, 638–641.
14. Monani, U.R., Coovert, D.D. and Burghes, A.H. (2000) Animal models of spinal muscular atrophy. *Hum. Mol. Genet.*, **9**, 2451–2457.
15. Park, G.H., Kariya, S. and Monani, U.R. (2010) Spinal muscular atrophy: new and emerging insights from model mice. *Curr. Neurol. Neurosci. Rep.*, **10**, 108–117.
16. Le, T.T., Pham, L.T., Butchbach, M.E., Zhang, H.L., Monani, U.R., Coovert, D.D., Gavrilina, T.O., Xing, L., Bassell, G.J. and Burghes, A.H. (2005) SMNDelta7, the major product of the centromeric survival motor neuron (*SMN2*) gene, extends survival in mice with spinal muscular atrophy and associates with full-length SMN. *Hum. Mol. Genet.*, **14**, 845–857.
17. Michaud, M., Arnoux, T., Bielli, S., Durand, E., Rotrou, Y., Jablonka, S., Robert, F., Giraudon-Paoli, M., Riessland, M., Mattei, M.G. *et al.* (2010) Neuromuscular defects and breathing disorders in a new mouse model of spinal muscular atrophy. *Neurobiol. Dis.*, **38**, 125–135.
18. Monani, U.R., Pastore, M.T., Gavrilina, T.O., Jablonka, S., Le, T.T., Andreassi, C., DiCocco, J.M., Lorson, C., Androphy, E.J., Sendtner, M. *et al.* (2003) A transgene carrying an A2G missense mutation in the SMN gene modulates phenotypic severity in mice with severe (type I) spinal muscular atrophy. *J. Cell Biol.*, **160**, 41–52.
19. Bowerman, M., Anderson, C.L., Beauvais, A., Boyl, P.P., Witke, W. and Kothary, R. (2009) SMN, profilin IIa and plastin 3: a link between the deregulation of actin dynamics and SMA pathogenesis. *Mol. Cell. Neurosci.*, **42**, 66–74.
20. Bowerman, M., Beauvais, A., Anderson, C.L. and Kothary, R. (2010) Rho-kinase inactivation prolongs survival of an intermediate SMA mouse model. *Hum. Mol. Genet.*, **19**, 1468–1478.
21. Riessland, M., Ackermann, B., Forster, A., Jakubik, M., Hauke, J., Garbes, L., Fritzsche, I., Mende, Y., Blumcke, I., Hahnen, E. *et al.* (2010) SAHA ameliorates the SMA phenotype in two mouse models for spinal muscular atrophy. *Hum. Mol. Genet.*, **19**, 1492–1506.
22. DiDonato, C.J., Lorson, C.L., De Repentigny, Y., Simard, L., Chartrand, C., Androphy, E.J. and Kothary, R. (2001) Regulation of murine survival motor neuron (Smn) protein levels by modifying Smn exon 7 splicing. *Hum. Mol. Genet.*, **10**, 2727–2736.
23. Singh, N.K., Singh, N.N., Androphy, E.J. and Singh, R.N. (2006) Splicing of a critical exon of human survival motor neuron is regulated by a unique silencer element located in the last intron. *Mol. Cell Biol.*, **26**, 1333–1346.
24. Cartegni, L., Wang, J., Zhu, Z., Zhang, M.Q. and Krainer, A.R. (2003) ESEfinder: a web resource to identify exonic splicing enhancers. *Nucleic Acids Res*, **31**, 3568–3571.
25. Cartegni, L., Hastings, M.L., Calarco, J.A., Stanchina, E. and Krainer, A.R. (2006) Determinants of exon 7 splicing in the spinal muscular atrophy genes, *SMN1* and *SMN2*. *Am. J. Hum. Genet.*, **78**, 63–77.
26. Hua, Y., Vickers, T.A., Okunola, H.L., Bennett, C.F. and Krainer, A.R. (2008) Antisense masking of an hnRNP A1/A2 intronic splicing silencer corrects SMN2 splicing in transgenic mice. *Am. J. Hum. Genet.*, **82**, 834–848.
27. Singh, N.N., Shishimorova, M., Cao, L.C., Gangwani, L. and Singh, R.N. (2009) A short antisense oligonucleotide masking a unique intronic motif prevents skipping of a critical exon in spinal muscular atrophy. *RNA Biol.*, **6**, 341–350.
28. Kashima, T., Rao, N. and Manley, J.L. (2007) An intronic element contributes to splicing repression in spinal muscular atrophy. *Proc. Natl Acad. Sci. USA*, **104**, 3426–3431.
29. Garbes, L., Riessland, M., Holker, I., Heller, R., Hauke, J., Trankle, C., Coras, R., Blumcke, I., Hahnen, E. and Wirth, B. (2009) LBH589 induces up to 10-fold SMN protein levels by several independent mechanisms and is effective even in cells from SMA patients non-responsive to valproate. *Hum. Mol. Genet.*, **18**, 3645–3658.
30. Ito, Y., Shibata, N., Saito, K., Kobayashi, M. and Osawa, M. (2010) New insights into the pathogenesis of spinal muscular atrophy. *Brain Dev.*
31. Pearn, J. and Hudgson, P. (1978) Anterior-horn cell degeneration and gross calf hypertrophy with adolescent onset. A new spinal muscular atrophy syndrome. *Lancet*, **1**, 1059–1061.
32. Workman, E., Saieva, L., Carrel, T.L., Crawford, T.O., Liu, D., Lutz, C., Beattie, C.E., Pellizzoni, L. and Burghes, A.H. (2009) A SMN missense mutation complements SMN2 restoring snRNPs and rescuing SMA mice. *Hum. Mol. Genet.*, **18**, 2215–2229.

Downloaded from https://academic.oup.com/hmg/article/19/21/4239/666050 by guest on 09 April 2024

33. Bouwsma, G. and Van Wijngaarden, G.K. (1980) Spinal muscular atrophy and hypertrophy of the calves. *J. Neurol. Sci.*, **44**, 275–279.
34. Pearn, J.H., Hudgson, P. and Walton, J.N. (1978) A clinical and genetic study of spinal muscular atrophy of adult onset: the autosomal recessive form as a discrete disease entity. *Brain*, **101**, 591–606.
35. Brahe, C., Servidei, S., Zappata, S., Ricci, E., Tonali, P. and Neri, G. (1995) Genetic homogeneity between childhood-onset and adult-onset autosomal recessive spinal muscular atrophy. *Lancet*, **346**, 741–742.
36. Butchbach, M.E., Edwards, J.D. and Burghes, A.H. (2007) Abnormal motor phenotype in the SMNDelta7 mouse model of spinal muscular atrophy. *Neurobiol Dis.*, **27**, 207–219.
37. Kong, L., Wang, X., Choe, D.W., Polley, M., Burnett, B.G., Bosch-Marce, M., Griffin, J.W., Rich, M.M. and Sumner, C.J. (2009) Impaired synaptic vesicle release and immaturity of neuromuscular junctions in spinal muscular atrophy mice. *J. Neurosci*, **29**, 842–851.
38. McGovern, V.L., Gavrilina, T.O., Beattie, C.E. and Burghes, A.H. (2008) Embryonic motor axon development in the severe SMA mouse. *Hum. Mol. Genet.*, **17**, 2900–2909.
39. Kariya, S., Park, G.H., Maeno-Hikichi, Y., Leykekhman, O., Lutz, C., Arkovitz, M.S., Landmesser, L.T. and Monani, U.R. (2008) Reduced SMN protein impairs maturation of the neuromuscular junctions in mouse models of spinal muscular atrophy. *Hum. Mol. Genet.*, **17**, 2552–2569.
40. Lefebvre, S., Burglen, L., Frezal, J., Munnich, A. and Melki, J. (1998) The role of the SMN gene in proximal spinal muscular atrophy. *Hum. Mol. Genet.*, **7**, 1531–1536.
41. Chen, H.H., Chang, J.G., Lu, R.M., Peng, T.Y. and Tarn, W.Y. (2008) The RNA binding protein hnRNP Q modulates the utilization of exon 7 in the survival motor neuron 2 (*SMN2*) gene. *Mol. Cell Biol.*, **28**, 6929–6938.
42. Watihayati, M.S., Fatemeh, H., Marini, M., Atif, A.B., Zahiruddin, W.M., Sasongko, T.H., Tang, T.H., Zabidi-Hussin, Z.A., Nishio, H. and Zilfalil, B.A. (2009) Combination of SMN2 copy number and NAIP deletion predicts disease severity in spinal muscular atrophy. *Brain Dev.*, **31**, 42–45.
43. Hofmann, Y., Lorson, C.L., Stamm, S., Androphy, E.J. and Wirth, B. (2000) Htra2-beta 1 stimulates an exonic splicing enhancer and can restore full-length SMN expression to survival motor neuron 2 (SMN2). *Proc. Natl Acad. Sci. USA*, **97**, 9618–9623.
44. Scharf, J.M., Endrizzi, M.G., Wetter, A., Huang, S., Thompson, T.G., Zerres, K., Dietrich, W.F., Wirth, B. and Kunkel, L.M. (1998) Identification of a candidate modifying gene for spinal muscular atrophy by comparative genomics. *Nat. Genet.*, **20**, 83–86.
45. Mende, Y., Jakubik, M., Riessland, M., Schoenen, F., Rossbach, K., Kleinridders, A., Kohler, C., Buch, T. and Wirth, B. (2010) Deficiency of the splicing factor Sfrs10 results in early embryonic lethality in mice and has no impact on full-length SMN/Smn splicing. *Hum. Mol. Genet.*, **19**, 2154–2167.
46. Gladman, J.T. and Chandler, D.S. (2009) Intron 7 conserved sequence elements regulate the splicing of the SMN genes. *Hum. Genet.*, **126**, 833–841.
47. Nagy, A., Gertsenstein, M., Vintersten, K. and Behringer, R. (2003) *Manipulating the Mouse Embryo: A Laboratory Manual*. Cold Spring Harbor Laboratory Press, Cold Spring Harbor, NY.
48. Haidet, A.M., Rizo, L., Handy, C., Umapathi, P., Eagle, A., Shilling, C., Boue, D., Martin, P.T., Sahenk, Z., Mendell, J.R. *et al.* (2008) Long-term enhancement of skeletal muscle mass and strength by single gene administration of myostatin inhibitors. *Proc. Natl Acad. Sci. USA*, **105**, 4318–4322.
49. Foley, K.P., McArthur, G.A., Queva, C., Hurlin, P.J., Soriano, P. and Eisenman, R.N. (1998) Targeted disruption of the MYC antagonist MAD1 inhibits cell cycle exit during granulocyte differentiation. *EMBO J.*, **17**, 774–785.
50. Ast, G. (2004) How did alternative splicing evolve? *Nat. Rev. Genet.*, **5**, 773–782.

Downloaded from https://academic.oup.com/hmg/article/19/21/4239/666050 by guest on 09 April 2024